# Spectroscopic detection of medium range order in device quality hydrogenated amorphous silicon, a-Si(H)

G. LUCOVSKY*, G. PARSONS, D. ZELLER, K. WU, B. PAPAS, J. WHITTEN, R. LUJAN[a], R. A. STREET[a]
*North Carolina State University Raleigh, N.C., 27695-8202, USA,*
[a]*The Palo Alto Research Company, a Xerox Company, Palo Alto, CA, 94303, USA*

Hydrogenated amorphous silicon, a-$Si_{1-x}H_x$, x ~0.1±0.02, has been used extensively in photo-voltaics and thin film transistors. This alloy has been deposited by the glow discharge method, remote plasma-enhanced chemical vapor deposition, and reactive magnetron sputtering with varying amounts of bonded-H determined by deposition precursors and substrate temperatures. Two conditions are required for ultra-low Si dangling bond densities of order 0.5 to 1x$10^{16}$ $cm^{-3}$: (i) a bonded monohydride, Si-H, concentration with 8 to 12 at.% H, and (ii) a deposition, and/or a post-deposition anneal at ~240 to 300°C. These conditions promote diffusion of H resulting in an optimized redistribution that reduces strain macroscopically, creating low Si dangling bond densities. Second derivative Si $L_{2,3}$ X-ray absorption spectroscopy has been used to confirm medium (or intermediate) range order extending beyond the short range order of continuous random networks through the observation of ligand field split features. These are associated with symmetry-adapted linear combinations of atomic states forming molecular orbital valence band states extending to at least 3rd Si neighbors. Medium range order can also be identified by complementary spectroscopic techniques, such as spectroscopic ellipsomentry (SE), and ultra-violet or X-ray photoemission spectroscopy (UPS or XPS).

(Received November 1, 2011; accepted November 23, 2011)

*Keywords*: a-Si, H, Spectroscopic detection, Medium range order

## 1. Introduction

Hydrogenated amorphous silicon, a-$Si_{1-x}H_x$, x ≈ 0.08 to 0.12, displays low dangling bond defect densities, and has become the preferred alloy for applications including the absorbing intrinsic or i-region in p-i-n photovoltaic (PV) devices, and the conducting channel in flat panel display thin film transistors (TFTs).[1)] Low defect density films have been deposited by the glow discharge (GD) method, remote plasma-enhanced chemical vapor deposition (RPECVD), and reactive magnetron sputtering (RMS). In addition to ~10 at.% bonded-H, these alloys require deposition temperatures ~240 to 275°C, and/or post-deposition annealing ~240 to 275°C.[2,3)] There has been much speculation about the near-neighbor bonding that promote a low-density of Si dangling bond defects. These extend into the mid-$10^{15}$ $cm^{-3}$ range and are comparable to defect densities in ultra-high purity crystalline Si and Ge.[4)] The role of bonded-H in mono-hydride Si-H arrangements is addressed in this article, and correlated with medium range (or intermediate range) order (MRO, or IRO), that extends beyond two-atom bond lengths, and three-atom bond-angle correlations, that define short range order (SRO) in the context of idealized continuous random networks (CRNs)[5,6)] MRO also includes at least third nearest-neighbor correlations giving rise to narrow distributions of dihedral angles, including their relative phase.[5)] Dihedral angle ordering is a necessary and sufficient condition for MRO in the a-Si(H) with 10 at.% bonded-H of this article. In crystalline solids dihedral angle correlations are periodic, but in a-Si(H) these are present in embedded intermediate-size locally rigid clusters with 10 to 15 Si atoms which are aperiodically distributed to minimize macroscopic strain.[7)]

X-ray absorption spectroscopy measurements at the Stanford Synchrotron Research Lightsource (SSRL),[8)] are combined H-atom diffusion measurements[9)] to explain low defect density a-Si:H alloys prepared by the 275°C GD method, and by RMS, but only after annealing to ~240°C.[4)] XAS spectra are compared in this article for two GD films: one deposited at a substrate temperature of 275°C with a low density of Si-atom dangling bonds, and the second deposited at 125°C, with Si polyhydride $(SiH_2)_n$ bonding and two orders of magnitude more Si dangling bonds.[3)]

## 2. Bonded-H in a-Si(H) Alloys

Relative concentrations of bonded-H have been determined by infrared absorption, with many of the relevant studies performed by the Lucovsky group at NC State University in the late 1980's.[2)] Reference 2 includes the variation of absorption constants for the Si-H bond-stretching vibration at ~2000 $cm^{-1}$, and three polyhydride group absorptions: (i) a bond-stretching mode at ~ 2090 $cm^{-1}$, and (ii) a scissors/wagging doublet at 890/845 $cm^{-1}$, each as a function of substrate temperature, $T_s$. By using peak absorption, or integrated total absorption standards, the relative fractions of Si-H, $[H]_M$, and $(SiH_2)_n$, $[H]_P$, are plotted as functions of $T_s$ in Fig. 1(a) of Ref. 2, for GD and RPECVD films. These plots are significantly different.

However, when GD and RPECVD results are re-plotted as $[H]_M$ and $[H]_P$ versus [H] in Fig. 1(b) of Ref. 2, the plots are the essentially the same. The bonded-H concentration, and not the $T_s$ determines the monohydride and polyhydride fractions for a given deposition process. This combination of plots in Ref. 2 establishes that the surface concentration of bonded-H required for a given concentration of bonded-H in the bulk film can be obtained by different deposition processes, and at different substrate temperatures, but this is must be followed by a post-deposition anneal to also yoield low dangling bond densities if the deposition temperature is below about 240°C.[4)]

Deposition, and/or post-deposition annealing in the temperature range between 240 and 275 to 300 °C is required to achieve low densities of dangling bonds for 10 at.% H a-Si(H) alloys. This has been addressed in Ref. 4, and criteria to distinguish between a "non-equilibrium" process, and a "relaxed, or reversible deposition" process are identified. These criteria are significant for results presented below, in particular the relationship between MRO and a H-diffusion process that reduces macroscopic strain.[9)]

Si $L_{2,3}$ soft X-ray absorption data for a-Si(H) and a-Si films and crystalline Si are compared. In the ionic limit, Si $L_{2,3}$ spectra are X-ray transitions from occupied, spin-orbit split Si $2p_{3/2}$ and $2p_{1/2}$ levels at ~ 99 eV to empty Si 3s and 3d states.[10)] Core holes in the Si 2p states play a significant role in these excitations. These are included using charge transfer multiplet (CTM) theory, represented symbolically in Eqns. 1(a) and 1(b). These apply more generally to final virtual bound 3s and 3d states:[10)]

$$2p^6 3s^0 \rightarrow 2p^5 3s^1 \quad 1(a), \text{ and } 2p^6 3d^0 \rightarrow 2p^5 3d^1 \quad 1(b).$$

Most importantly, the observation of $2p^6 3d^0 \rightarrow 2p^5 3d^1$ transitions requires MRO order that includes at least third nearest-neighbor correlations defining discrete dihedral angles.[8)] These correlations are revealed in valence band spectra as critical point structures. They are associated with symmetry adapted linear combinations (SALC) of atomic states including the splitting of d-state contributions in the local field tetrahedral symmetry at the Si-atom bonding sites.[11)] This scale of MRO is sufficient for a ligand field splitting, ΔLF, to be detected in Si $L_{2,3}$ spectra. The valence band spectrum of a-Si with only SRO (bond-lengths and bond-angles) is comprised of two features associated respectively with Si 3s and 3p atomic states[12)], whilst the spectrum for hydrogenated amorphous Si with 10 at.% H, displays additional features associated with molecular orbital states associated with SALCs of atomic states, thereby revealing MRO.[13)] MRO, as well as long range periodic order (LRO), is *inherent* in single crystalline and nano-crystalline Si, but is subject to periodicity which produces cancellations for some symmetry allowed transitions similar to what happens in X-ray diffraction.[14)]

When core holes and basis set wave functions symmetry-adapted for tetrahedral bonding of Si are included, each CTM transition in Eqn. (1) is from an "s-like" ground state to "p-like' final states. Ground states are non-degenerate singlet $^1A_1$ terms, and final states are triply degenerate singlet $^1T_2$ terms.[7)] Photon absorption requires a non-zero matrix element, $< {}^1T_2 \mid \mathbf{e}\mathbf{r} \mid {}^1A_1 > \neq 0$, where $\mathbf{e}\mathbf{r}$ is the dipole operator, and is dependent only on the radial part of the wave function.

In the presence of MRO, there is a spectroscopically detectable ligand field splitting, ΔLF, with six terms for each of the transitions in Eqns. 1(a) and 1(b). However, in the absence of MRO, there are only two 2p to 3s transition features, each symmetric and separated by the ground state Si $2p_{3/2}$ - Si $2p_{1/2}$ spin-orbit splitting of 0.6±0.1 eV. These two absorptions result from bonding correlations that include only nearest- and next-nearest neighbor SRO bond-lengths and bond-angles. The x-axis photon energies in all plots have been scaled linearly from the soft X-ray regime, ~98 eV to ~102 eV, to the visible-vacuum ultra-violet (vis-VUV) regime, from 2.3 eV to 6.3 eV to provide comparisons with other experiments.[11)] This calibration is based on a comparison between the 2nd derivative c-Si visible-vacuum-ultra-violet (vis-VUV) expsilon 2 spectra extracted from spectroscopic ellipsometry (SE), and the crystalline Si XAS $L_{2,3}$ spectrum, The ligand field splitting of Si d-states in tetrahedral bonding coordinations contribute to the molecular orbital ground states of the valence band, and as such are revealed in transitions to virtual bound states of the conduction band.[11)]

Fig. 1 is a comparison of the XAS Si $L_{2,3}$ spectra for (i) crystalline Si (c-Si) and (ii) the 275 °C GD a-Si(H) film. Qualitative features in the two spectra are similar including the edge at ~2.6 eV corresponding to the onset of 2p to 3s transitions, and (ii) a weaker feature at ~3.7 eV heralding the onset of 2p to 3d transitions. Two pairs of features, separated by an energy equal to the Si 2p spin-orbit splitting of 0.6±0.1 eV, identify the same ligand field spitting of 1.7±0.1 eV for c-Si and the GD 275°C a-Si(H). This demonstrates that the GD 275°C a-Si(H) thin films with ~10 at.% bonded-H have MRO extending into the regime of discrete dihedral angles.

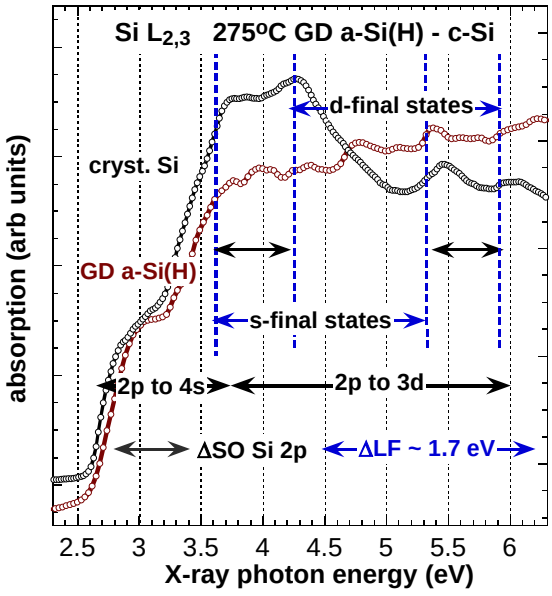


*Fig. 1. Si $L_{2,3}$ spectra for crystalline Si, and the 275 °C GD a-Si(H) film.*

Fig. 2 indicates this scale of order in a schematic diagram. This includes the Si-H bond, and two additional 'layers' of Si atoms the include discrete dihedral angles. The local structure has essentially the same SRO and MRO as crystalline and nano-crystalline Si.

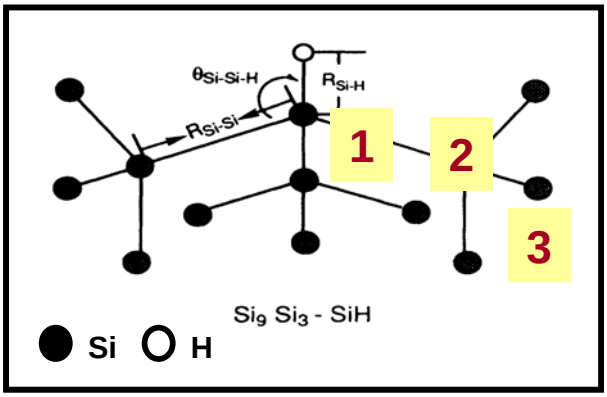


*Fig. 2. Schematic representation of MRO at Si-H site, extending to 3rd nearest neighbors to the H-atom, and including discrete values of the dihedral angles.*

Fig. 3 compares second derivative Si $L_{2,3}$ X-ray spectra for the 275C GD film and c-Si, complementing the two the Si $L_{2,3}$ traces in Fig. 1. Qualitative features in the spectra are similar, but details differ significantly. The c-Si spectrum shows more detail in the 2p to 3s spectral regime, whilst the a-Si(H) spectrum shows more strong features in the 2p to 3d spectral regime. Differences in the 2p to 3d regime are explained by noting that the a-Si(H) portion of the spectrum reflects only MRO order, and is not subject to cancellations derived from the long range periodicity in the c-Si spectrum.[14] Fewer features in the c-Si $L_{2,3}$ spectrum are then analogous to forbidden reflections in X-diffraction.

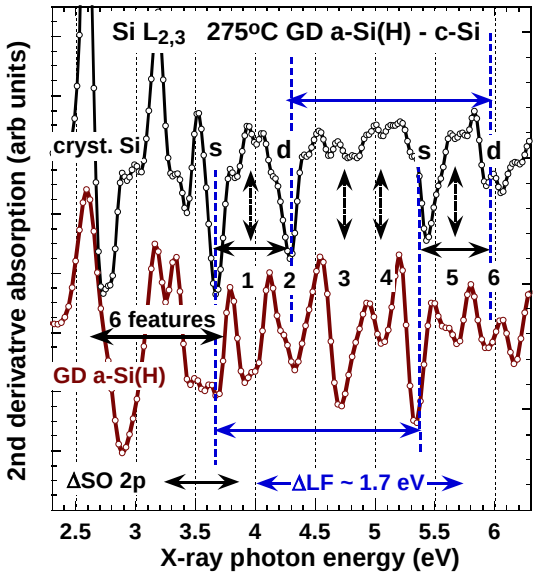


*Fig. 3. Second derivative $L_{2,3}$ X-ray spectra for crystalline Si, and the 275 °C GD a-Si(H) film.*

Fig. 4 displays Si $L_{2,3}$ second derivative spectra for (i) the 125 °C GD a-Si(H) film, and (ii) an a-Si film prepared by RPECVD. Each of these spectra displays the same two symmetric features centered, at ~2.76 and 3.40 eV in the $2p^6 3s^0$ → $2p^5 3s^1$ portion of the spectrum. These are separated by the Si 2p spin-orbit splitting of 0.6±0.1 eV. These two features in Fig. 4 for the a-Si film are "functionally: equivalent to the single feature centered at ~3 eV in vis-VUV data.[15] The absence of distinct features between 3.6 eV and 5.6 eV in this figure, and Fig. 1 of Ref. 11 indicates the no ligand field splitting, and hence no MRO order in a-Si films deposited at room temperature. The absence of MRO in the GD 125 °C film derives from the absence of dihedral angle correlations and MRO for the disordered polyhydride $(SiH_2)_n$ chains.[5]

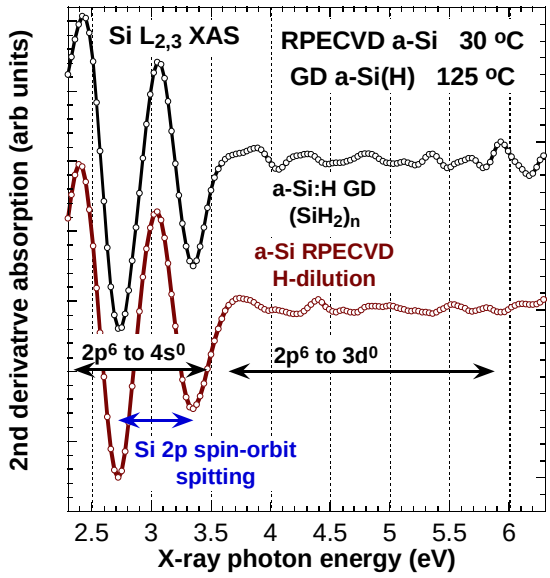


*Fig. 4. Si $L_{2,3}$ second derivative spectra for (i) the 125 °C GD a-Si(H) film, and (ii) an a-Si film prepared by RPECVD.*

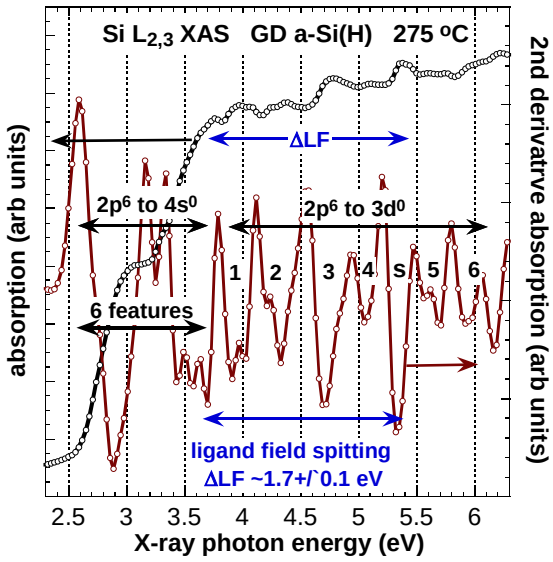


*Fig. 5. Si $L_{2,3}$ and second derivative spectra for the 275 °C GD a-Si(H) film. and crystalline Si.*

Si $L_{2,3}$ and second derivative Si $L_{2,3}$ spectra for a-Si(H) film GD deposited at 275°C are displayed in Fig. 5. The second derivative spectrum is markedly different than the 125°C spectrum in Fig. 3. Each set of the CTM transitions in Eqns. 1 and 2 has six terms, and these are more distinct in the second derivative spectrum. The detection of six final "d-state" $^1T_{2g}$ terms is definitive evidence for a ligand field splitting and MRO that extends to at least three-atom dihedral angle correlations as indicated in Fig. 2.

## 4. Discussion

The most significant aspect of the experimental results is the relationship between the MRO in the GD a-Si(H) films deposited at 275°C, and the low defect density that is enabling for important applications in a-Si(H) thin films in PV that TFT applications. The MRO extends into the regime of discrete dihedral angles and has been illustrated schematically in Fig. 2. The low defect density and structural order arise from the ability for hydrogen to diffuse within the a-Si matrix at the higher temperatures, 240 to 300°C for the samples in this article, and in Ref. 4, but not at 125°C. This diffusive motion permits aperiodic structural relaxations extending to 3rd next-nearest neighbor Si atoms in the 275°C film. This *atomic volume amplification factor* for 10 at.% H in the Si-H groups, exceeds the critical volume percolation threshold of 16.5%,[16] This means a relatively small concentration of Si-H bonds promotes macroscopic strain reduction throughout the entire film, but not necessarily reduction of the local strain within the MRO cluster. When applied to films produced with H-dilution with 5-6 % bonded-H in monohydride arrangements, this percolation threshold for local strain relief is exceeded as well, explaining the low defect densities in these films.[17]

In another paper,[18] a displace H-transport mechanism for the Staebler-Wronski effect (SWE) has been presented. This involves a displacive transport of a H-atom from the MRO cluster in Fig. 2 to a strained Si-Si bonding of the encapsulating network that has trapped a photo-generated hole. The precursor state for the SWE is MRO cluster, and a strained neutral Si-Si bond of the encapsulating network. The low density of defects in a-Si(H) with ~10at.% H are pre-existing defects created by bond-stretching vibrations of the Si-H vibration, the same way that vacated O-atoms sites are created in $SiO_2$ films and glasses.

**Acknowledgements**

The authors acknowledge support from the AFOSR and DTRA. The unique character of Beam Line facilities at SSRL in Menlo Park, CA is gratefully acknowledged. Most importantly this paper was finalized on the last day of my dear wife's life, September 10, 2011. She was the "love of my life" and her tenderness and constant support always shown through. She lives in my heart forever, and this paper, along with another one in these proceedings is a testimony to her courage that has continued to sustain me.

## References

[1] P.G. LeComber, J. Non-Cryst. Solids **115**, 1 (1989).
[2] G. Lucovsky, B.N. Davidson, G.N. Parsons C. Wang, J. Non-Cryst. Solids **114**, 178 (1989).
[3] R.A. Street, D.K. Beigelsen, J.C. Knights, Phys. Rev. B **24**, 969 (1981).
[4] G.N. Parsons, C. Wang, M.J. Williams, Appl. Phys. Lett. **56**, 1985 (1990).
[5] G. Lucovsky, F.L. Galeener, J. of Non-Cryst. Solids **35 & 36,** 1209 (1980).
[6] R. Zallen, The Physics of Amorphous Solids (John Wiley, New York, 1983).
[7] J. L. Whitten, et al., J. Vac. Sci..Technol. B **20**, 1710 (2002).
[8] G. Lucovsky, K.B. Chung, L. Miotti, et al., Solid State Electronics **53**, 1273 (2009).
[9] J.C. Knights in The Physics of Amorphous Silicon I, Eds. J.D. Joannopoulos and G. Lucovsky (Springer-Verlag, Berlin, 1984) Chap. 2.
[10] F.M.F. de Groot, J.C. Fluggle, et al., Phys. Rev. **41**, 928 (1990).
[11] F.A. Cotton, Chemical Applications of Group Theory, 2nd Ed. (Wiley Interscience, New York, 1963) Chapter 8.
[12] L. Ley, S. Kowalczyk, and R. Pollak, Phys. Rev. Lett. **29**, 1068 (1972).
[13] B. von Roeden, L. Ley, and M. Cardona, Phys. Rev. Lett. **39**, 1576 (1977).
[14] C. Kittel, Introduction to Solid State Physics, 8th Edition (John Wiley, New York, 2005),
[15] B. Kramer, K. Maschke, P. Thomas, phys. stat. sol. (b) **49**, 525 (1972).
[16] H. Scher, R. Zallen, J. Chem. Phys. **53**, 3759 (1970).
[17] S. Guha, J. Yang, D. L. Williamson, et al., Appl. Phys. Lett. **74**, 1860 (1999).
[18] G. Lucovsky, et al., Paper ID. 1312 of these proceedings.
[19] G. Lucovsky, et al., Paper ID. 1315 of these proceedings.

*Corresponding author: lucovsky@ncsu.edu